

31 Abstract

32 *Searches for phosphine in Venus' atmosphere have sparked a debate. Cordiner et al. 2022*
 33 *analyse spectra from the Stratospheric Observatory For Infrared Astronomy (SOFIA) and infer*
 34 *<0.8 ppb of PH₃. We noticed that some spectral artefacts arose from non-essential calibration-*
 35 *load signals. By-passing these signals allows simpler post-processing and a 5.7 σ candidate*
 36 *detection, suggesting ~3 ppb of PH₃ above the clouds. Compiling six phosphine results hints at*
 37 *an inverted abundance trend: decreasing above the clouds but rising again in the mesosphere*
 38 *from some unexplained source. However, no such extra source is needed if phosphine is*
 39 *undergoing destruction by sunlight (photolysis), to a similar degree as on Earth. Low phosphine*
 40 *values/limits are found where the viewed part of the super-rotating Venusian atmosphere had*
 41 *passed through sunlight, while high values are from views moving into sunlight. We suggest*
 42 *Venusian phosphine is indeed present, and so merits further work on models of its origins.*

43 Plain Language Summary

44 *Cordiner et al. find no phosphine in Venus' atmosphere, using the airborne SOFIA telescope.*
 45 *By-passing some instrumental effects, we extract a detection with 5.7 σ -confidence from the same*
 46 *data. We can resolve the tension between high and low PH₃ abundance values by noticing that*
 47 *the former are from 'mornings' in Venus' atmosphere and the latter from 'evenings'. Sunlight*
 48 *reduces the amount of phosphine in Earth's atmosphere by an order of magnitude, so similarly*
 49 *on Venus, we might expect lower abundances in data taken when the part of the atmosphere*
 50 *observed has passed through sunlight. If the six available datasets can be reconciled in this way,*
 51 *further modelling of possible sources of PH₃ (e.g. volcanic, disequilibrium chemistry, extant life)*
 52 *seem worthwhile.*

53 1 Introduction

54 Phosphine, if present in Venus' atmosphere, would be unexpected on an oxidised planet.
 55 Greaves et al. (2021) searched for PH₃ absorption at 1 mm wavelength, testing the concept that
 56 this molecule may be a biosignature when seen in anoxic environments. The unexpected
 57 detection-candidates from *JCMT* and *ALMA* have stimulated much community work on robust
 58 spectral processing, and on other methods to detect PH₃ at Venus, mostly proving negative
 59 except for an in-situ mass-spectrometry recovery (Mogul, Limaye, Way, et al., 2021).
 60 Particularly deep (above-cloud) limits have been set by infrared spectroscopy (Encrenaz et al.,
 61 2020; Trompet et al., 2020).

62 We comment here on the findings of Cordiner et al. (2022), hereafter C22, who present a
 63 deep upper limit from PH₃ observations with the *GREAT* instrument on *SOFIA*. They propose
 64 that *all* the candidate detections of phosphine in Venus' atmosphere could in fact be null results,
 65 given the complexity of the challenging observations – although their Figure 1 omits findings by
 66 Greaves et al. (2022), our work after calibration and contamination issues were fully resolved,
 67 where we find self-consistent 6-8 σ detections for the PH₃ J=1-0 line from *JCMT* and *ALMA*.

68 The C22 observations are of the rotational transitions J=4-3 and 2-1 (around 1 and 0.5
 69 THz), uniquely accessible to the *SOFIA* airborne telescope, and complementary to the existing
 70 J=1-0 spectra (at 0.27 THz). From their J=4-3 data processing, C22 find an upper limit of 0.8 ppb
 71 of PH₃, applicable to most of the planet and 75+ km altitudes, while their J=2-1 results suggest
 72 ~2.3 ppb could be present but only with 1.5 σ confidence. These abundances are difficult to

73 reconcile with ~20 ppb levels from the J=1-0 data, without invoking strong temporal-variations
 74 or steep gradients over the slightly different altitudes these lines trace.

75 **2 Materials and Methods**

76 C22 note the existence in the *GREAT* spectra of quasi-periodic fringe patterns, due to
 77 standing waves between optical elements and to frequency-dependent gain factors used in
 78 calibration. Their calibration to antenna temperatures T_A follows the standard method of dividing
 79 the power difference of on- and off-Venus spectra by the power difference of hot and cold
 80 calibration-load signals, and then multiplying by the temperature difference of the hot and cold
 81 loads. We noticed that much of the fringing is introduced because the standing waves differ
 82 when observing the sky and the calibration loads. However, calibration to T_A is not essential in
 83 measuring the line-to-continuum ratios, l/c , from which abundances derive. In the case of the
 84 PH_3 J=4-3 line components (seen by the “4G2 pixel”), an alternative is

$$85 \quad l/c = (On_{line} - Off_{line}^*) / [0.5(On - Off)] \quad [1]$$

86 where On and Off are the spectra on Venus and on adjacent blank sky, the subscript *line* indicates
 87 the broadband signals have been subtracted, and Off_{line}^* represents the instrumental line-signal
 88 that *GREAT* would see for a featureless patch of sky of similar brightness to Venus. Off_{line}^* was
 89 generated by multiplying Off_{line} by a factor ~1.05 and adjusting this scalar until the residual
 90 ($On_{line} - Off_{line}^*$) was minimised – that is, the procedure tests the null hypothesis, that no
 91 absorbing gases are present. Smooth fits to On and Off (the continuum signals) were used in the
 92 denominator of [1] to further minimise noise. The factor of 0.5 arises because *GREAT* is a
 93 double-sideband instrument with approximately equal sideband gains (see C22), and so records
 94 the planetary continuum twice. The Eq. [1] method has worked well here for PH_3 J=4-3, reaching
 95 a similar noise level to C22, but our approach failed for the PH_3 J=2-1 line-pair (“4G1 pixel”)
 96 because the ripples differ between On_{line} and Off_{line} .

97 Remaining ripples in the J=4-3 spectra were then removed by a one-stage Fourier
 98 process, contrasting to the iterative 7-step Lomb-Scargle periodogram approach used by C22 (or
 99 traditional polynomial fitting, which is less useful for spectra with many ripples). Both we and
 100 C22 similarly “masked” the spectral regions where the four PH_3 components lie, to avoid fitting
 101 real lines as if they are ripples. C22’s periodogram method works intrinsically on masked data,
 102 while we interpolated across the line regions with quadratic fits anchored on adjacent spectral
 103 pixels. We used 3-sigma cuts in Fourier space, with features above these cuts inverse-Fourier-
 104 transformed to create a family of model sinusoids. Subtracting these model baselines yields well-
 105 flattened spectra (Figures 1a, 1b). Finally we “stack” the 24 samples of PH_3 absorption in the
 106 data (Figure 1c), namely from the 6 observations and their 4 spectral sections covering the J=4-3
 107 components, as these are of similar intrinsic line-depth (see Figure 3 in C22). Two of the PH_3
 108 features are close together (Figure 1b), and so to avoid duplications, we replaced the secondary
 109 occurrences with noise values from elsewhere in the spectrum, before making the final stack.

110 Several robustness checks were run, exploring possible processing issues.

- 111 • The net result could be dominated by a few strong artefacts. This was found not to be the
 112 case, with the line-integrals from the 24 samples following an approximately normal
 113 distribution. The result is also robust to removing a few points. For example, the final
 114 observation (#040402) was the noisiest, and removing all these samples from the stack shifts
 115 the net line-integral by only -20%.

- 116 • There could be terrestrial atmospheric signals in the band, that affect the validity of
 117 minimising the numerator in Eq. [1]; in particular, C22 note two frequencies where there may
 118 be O₃ absorption. We re-calculated the scalar used in Eq. [1] with the O₃ regions blanked,
 119 and found negligible change (around 1% reduction in noise).
- 120 • The interpolation across the PH₃ line-regions might not be following the correct trend,
 121 potentially always producing negative residuals that mimic absorption lines. We tested this
 122 by re-running the processing identically, but shifting the spectral sections to parts of the band
 123 without phosphine features. From 50 tests, none produced a result like Figure 1c, namely a
 124 “fake” absorption that is the only feature, centrally placed, and of comparable width to line
 125 models (see below).

126

127 **3 Results**

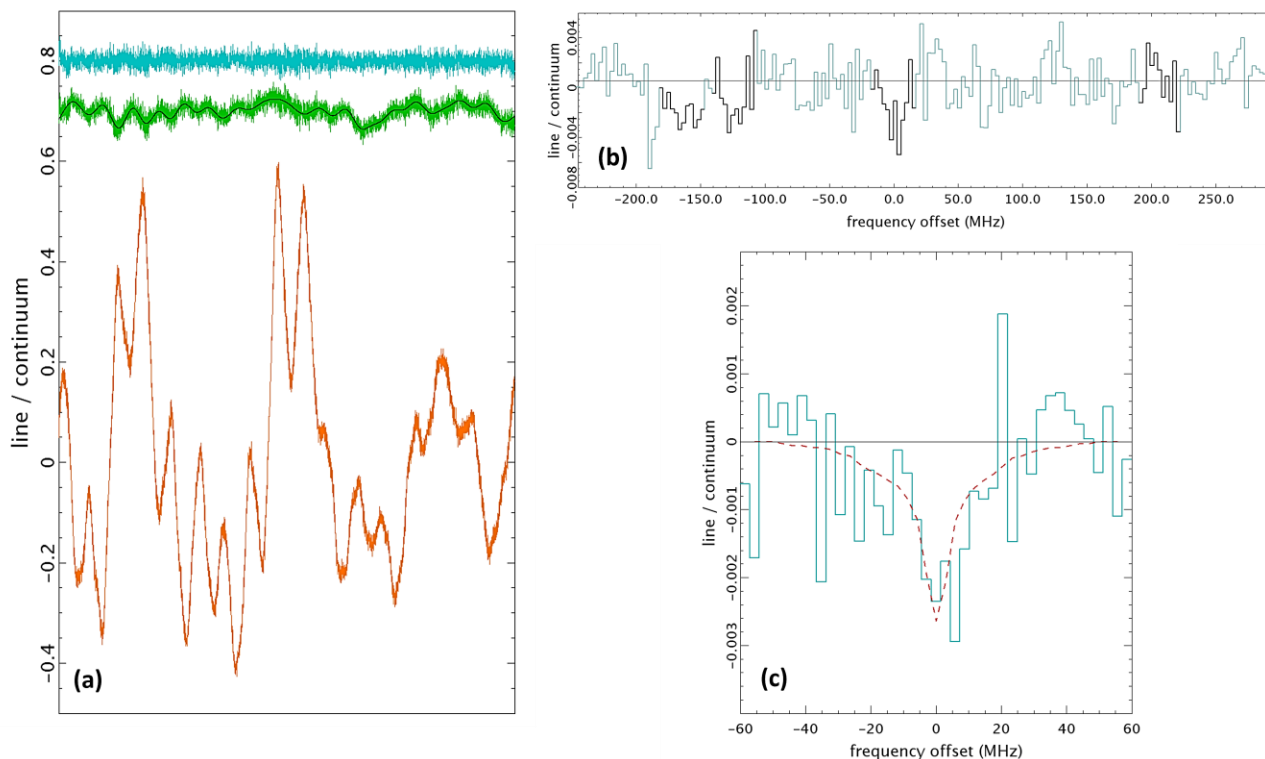
128 Three of the four expected PH₃ J=4-3 components are visible when all the observations
 129 are co-added (Figure 1b), while only one component was apparent in Figure 3 of C22. In Figure
 130 1c, our final stacked spectrum indicates an overall 5.7 σ detection of PH₃ J=4-3, when integrated
 131 over ± 17 MHz (the masked region). This confidence level changes marginally (by $\pm 0.4\sigma$) if a
 132 different range of spectral pixels is used to calculate the zero-level.

133 We then modelled our net spectrum using the same online tool as C22. We ran a model
 134 for 1 ppb of phosphine and scaled it linearly for different abundances, and then calculated a
 135 reduced-chi-squared statistic to assess goodness of fit. Figure 1c illustrates that 3 ppb of PH₃
 136 provides a good match to the observed line, with χ^2_r of 0.75. (The uncertainties used in χ^2_r were
 137 generated per spectral pixel from the internal data dispersion.) We consider that fitting the
 138 stacked spectrum better mitigates against artefacts, compared to matching the individual
 139 components (Figure 1b) against the model. For example, inserting a single positive “spike” near
 140 the highest-frequency component (Figure 1b) was found to significantly reduce the inferred PH₃
 141 abundance, as the χ^2_r test attempts to minimise the discrepancy of positive data against a
 142 negative model-line. As a positive feature does appear here in this part of C22’s spectrum (their
 143 Figure 3), this could have driven their upper limit down to the ≤ 0.8 ppb they obtain. However,
 144 we do not rule out an abundance as low as 0.8 ppb, which is at the lower 99% confidence-bound
 145 in our χ^2_r tests. We also note that C22 estimated ~ 2.3 ppb from their PH₃ J=2-1 spectrum, albeit
 146 at only +1.5 σ confidence, and this estimate is compatible with our 3 ppb result.

147 C22 (Figure S4) find that altitudes around ~ 80 km are the best-sampled at the PH₃ J=4-3
 148 line-frequency; our recovery here is consistent with the model that we both use, and with the
 149 predicted short lifetime of PH₃ above ~ 80 km (Bains, Petkowski, Seager, et al., 2021). Altitudes
 150 are however uncertain because the PH₃-CO₂ pressure-broadening coefficient has not been
 151 experimentally verified. We also note that all GHz/THz data are limited by the spectral span that
 152 can be recovered. Here, any absorption wider than ~ 200 MHz leads to merged PH₃ J=4-3
 153 components, and so any phosphine signatures below ~ 70 km (roughly cloud-top level) are lost.

154 *Figure 1. The process of extracting the PH₃ J=4-3 signal from the GREAT data is illustrated.*
 155 *Panel (a) illustrates processing of 6000 spectral pixels from observation #040093 from the first*
 156 *SOFIA flight (the reference spectral pixel is mid-band; vertical offsets are for clarity only). The*
 157 *lower orange histogram is from a standard On-Off processing; the middle green histogram is the*
 158 *result after applying the Eq.[1] step, and is overlaid with the Fourier-derived trend (black*
 159 *curve); the top blue histogram is the flattened output after subtracting this trend. In panel (b),*

160 *the blue histogram is the unweighted average of all six observations made over the three flights,*
 161 *with the sections containing the four PH₃ J=4-3 components highlighted in black. The spectral*
 162 *pixels are binned in groups of 12 in (b) and (c) to improve clarity, and the thin black lines show*
 163 *the zero-level correction made between (b) and (c). Panel (c) shows (blue histogram) the*
 164 *unweighted stack of all 24 spectral sections containing PH₃ J=4-3 features. The dashed red*
 165 *curve is a model for 3 ppb of phosphine, generated via the Planetary Spectrum Generator (PSG)*
 166 *(<https://psg.gsfc.nasa.gov/index.php>) following C22. The four line-components from the PSG*
 167 *model were masked and stacked similarly to the data.*



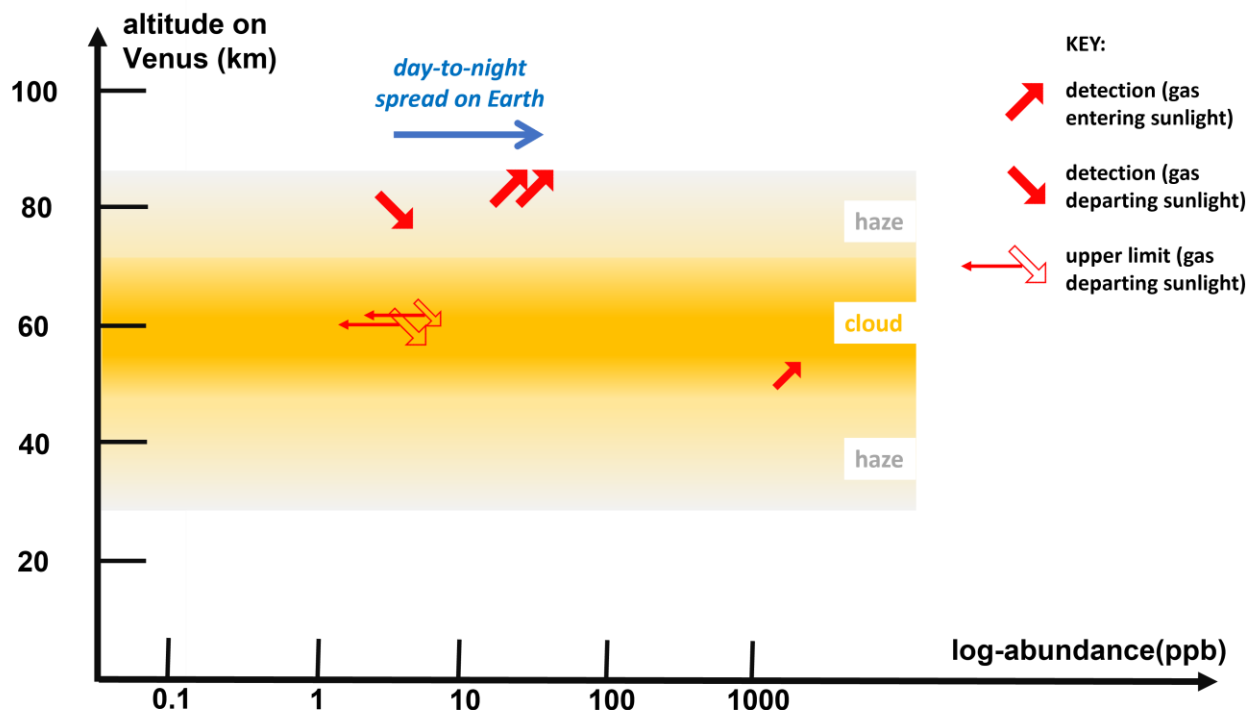
168 **4 Discussion**

169 Debates continue about the best methods to acquire and process deep GHz/THz spectra
 170 of Venus. These observations are very challenging in dynamic range, as Venus is so bright,
 171 revealing “ripples” in spectral baselines that are not evident in more typical telescope usage.
 172 Depending on preferred approaches, different authors argue for between zero and three published
 173 detections of rotational (J) transitions of PH₃.

174 We can compare results from the data discussed here with the outcomes of other searches
 175 for phosphine at Venus, and assess whether this results in a plausible altitude profile of the
 176 molecule (Figure 2). The trend found by connecting the results from six searches for phosphine
 177 appears as an upwards decline that then reverses, i.e. PH₃ that is depleted somewhere between
 178 ~50 km and ~80 km. This is hard to explain in the absence of a chemical route to reform the
 179 molecules, or a new mesospheric source. The order-of-magnitude contrast between some of the
 180 candidate detections and the upper limits has led to doubts over the presence of phosphine.

181 However, we noticed that this divide is also between observations made when the
 182 ‘morning’ versus the ‘evening’ sides of Venus’ atmosphere were targeted – and this is relevant in
 183 gas-mixing processes (e.g. (Lefèvre et al., 2022)). Where the gas observed on Venus has
 184 travelled through sunlight and is descending towards the night-side of the planet, we detect at
 185 most the ~ 3 ppb of phosphine estimated here. In contrast, where gas is rising into sunlight, we
 186 observe $\geq \sim 20$ ppb of PH_3 . Hence photolysis – similar to the observed destruction of terrestrial
 187 phosphine by sunlight (Sousa-Silva et al., 2020) – could explain the split between high and low
 188 phosphine abundances observed on Venus. It is striking that this evening/morning difference is
 189 comparable in magnitude to the factor ~ 10 difference over night/day for phosphine in the Earth’s
 190 atmosphere (Glindemann et al. 1996; noting absolute abundances are much lower on Earth).

191 *Figure 2. The trend of phosphine abundances by altitude is sketched. Symbols indicate candidate*
 192 *detections plus best upper limits for phosphine abundances. Rising arrows indicate observations*
 193 *made where the super-rotating atmosphere was rising into sunlight and falling arrows indicate*
 194 *observations made where the atmosphere was descending towards the nightside (see key). Large*
 195 *and small symbols indicate that a large fraction of the planet area was observed, or that a small*
 196 *region was sampled, respectively. Abundance estimates are, from top: ~ 20 , 25 ppb from J=1-0*
 197 *data (via (Greaves et al., 2022) and with altitude proposed by C22); 3 ppb from J=4-3 data (this*
 198 *work; beam centred on the evening side); < 7 ppb at 62 km from $4 \mu\text{m}$ spectra (Trompet et al.,*
 199 *2020: low-latitude data to best match whole-planet studies); < 5 ppb at 60 km from $10 \mu\text{m}$*
 200 *spectra (Encrenaz et al., 2020: latitudes within $\pm 50^\circ$); ~ 2 ppm at 51 km from Pioneer-Venus*
 201 *in-situ sampling during descent (Mogul, Limaye, Way, et al., 2021). The blue arrow indicates the*
 202 *ten-fold increase of terrestrial phosphine from day to night (Glindemann et al. 1996) – note the*
 203 *arrow’s plotted position is arbitrary; Earth hosts much lower PH_3 than Venus.*



205 5 Conclusions

206 The question regarding phosphine in Venus' atmosphere is likely to be debated for some
 207 time. A further *JCMT* survey is ongoing (see [https://www.eaobservatory.org/jcmt/science/large-](https://www.eaobservatory.org/jcmt/science/large-programs/jcmt-venus-monitoring-phosphine-and-other-molecules-in-venuss-atmosphere/)
 208 [programs/jcmt-venus-monitoring-phosphine-and-other-molecules-in-venuss-atmosphere/](https://www.eaobservatory.org/jcmt/science/large-programs/jcmt-venus-monitoring-phosphine-and-other-molecules-in-venuss-atmosphere/); PI. D.
 209 Clements) and is producing open-source data that should yield more definitive answers – in
 210 particular, that team is now processing broadband spectra that can sample the cloud decks. The
 211 most direct answer regarding phosphine could come from new in-situ sampling, potentially with
 212 the addition of one laser channel to the Venus Tunable Laser Spectrometer (VTLS) instrument
 213 on-board the *DAVINCI* descent probe (Garvin et al. 2022).

214 The origins of any phosphine present are also debated, and most scenarios are hard to test
 215 for lack of some contextual data. For example, it seems only extraordinary volcanic activity
 216 could make ~ppb-level phosphine (Bains et al., 2022) but vulcanism on Venus is not well
 217 understood. In some new avenues, (Ferus et al., 2022) discuss abiotic routes to phosphine
 218 involving redox disequilibrium, while others (Bains, Petkowski, Rimmer, et al., 2021; Mogul,
 219 Limaye, Lee, et al., 2021) explore phototrophic life and the habitability of the clouds. We
 220 conclude that establishing an improved PH₃ altitude-profile is worthwhile to test these new
 221 models of origins.

222 Acknowledgments

223 This work is based in part on observations made with the NASA/DLR *Stratospheric Observatory*
 224 *for Infrared Astronomy (SOFIA)*. *SOFIA* is jointly operated by the Universities Space Research
 225 Association, Inc. (USRA), under NASA contract NNA17BF53C, and the Deutsches SOFIA
 226 Institut (DSI) under DLR contract 50 OK 2002 to the University of Stuttgart. We thank Helmut
 227 Wiesemeyer, Martin Cordiner and staff at the *SOFIA* Science Center for their invaluable help.
 228

229 Open Research

230 The SOFIA Level 1 data are available under project id 75_0059_1 through the public data
 231 archive at <https://irsa.ipac.caltech.edu/applications/sofia>. The custom software to generate the
 232 data shown in the figures is supplied at <https://zenodo.org/record/7692288#.ZAC363bP3IU>. The
 233 script requires the UK-Starlink software (Currie et al., 2014) which is currently supported by the
 234 East Asian Observatory and available at <https://starlink.eao.hawaii.edu/starlink/2021ADownload>.

236 References

- 237 Bains, W., Petkowski, J. J., Seager, S., Ranjan, S., Sousa-Silva, C., Rimmer, P. B., et al. (2021).
 238 Phosphine on Venus Cannot be Explained by Conventional Processes. *Astrobiology*, 21(10),
 239 1277–1304. Retrieved from <https://ui.adsabs.harvard.edu/abs/2020arXiv200906499B>
 240 Bains, W., Petkowski, J. J., Rimmer, P. B., & Seager, S. (2021). Production of Ammonia Makes
 241 Venusian Clouds Habitable and Explains Observed Cloud-Level Chemical Anomalies.
 242 *Proceedings of the National Academy of Science*, 118(52).
 243 Bains, W., Shorttle, O., Ranjan, S., Rimmer, P. B., Petkowski, J. J., Greaves, J. S., & Seager, S.
 244 (2022). Constraints on the production of phosphine by Venusian volcanoes. *Universe*, 8(1),
 245 54.
 246 Cordiner, M. A., Villanueva, G. L., Wiesemeyer, H., Milam, S. N., de Pater, I., Moullet, A., et al.

- 247 (2022). Phosphine in the Venusian Atmosphere: A Strict Upper Limit from SOFIA GREAT
248 Observations. *Geophysical Research Letters*, e2022GL101055.
- 249 Currie, M. J., Berry, D. S., Jenness, T., Gibb, A. G., Bell, G. S., & Draper, P. W. (2014). Starlink
250 software in 2013 (Vol. 485, p. 391).
- 251 Encrenaz, T., Greathouse, T. K., Marcq, E., Widemann, T., Bézard, B., Fouchet, T., et al. (2020).
252 A stringent upper limit of the PH₃ abundance at the cloud top of Venus. *Astronomy &*
253 *Astrophysics*, 643, L5.
- 254 Ferus, M., Cassone, G., Rimmer, P., Saija, F., Mráziková, K., Knížek, A., & Civiš, S. (2022).
255 Abiotic chemical routes towards the phosphine synthesis in the atmosphere of Venus. In
256 *European Planetary Science Congress* (pp. EPSC2022-198).
- 257 Garvin, J. B. et al. (2022) 'Revealing the Mysteries of Venus: The DAVINCI Mission', The
258 *Planetary Science Journal*, 3(5), p. 117. doi: 10.3847/psj/ac63c2.
- 259 Glindemann, D., Bergmann, A., Stottmeister, U., & Gassmann, G. (1996). Phosphine in the
260 lower terrestrial troposphere. *Naturwissenschaften*, 83(3), 131-133
- 261 Greaves, J. S., Richards, A. M. S., Bains, W., Rimmer, P. B., Sagawa, H., Clements, D. L., et al.
262 (2021). Phosphine gas in the cloud decks of Venus. *Nature Astronomy*, 5(7), 655–664.
- 263 Greaves, J. S., Rimmer, P. B., Richards, A., Petkowski, J. J., Bains, W., Ranjan, S., et al. (2022).
264 Low levels of sulphur dioxide contamination of Venusian phosphine spectra. *Monthly*
265 *Notices of the Royal Astronomical Society*, 514(2), 2994–3001.
266 <https://doi.org/10.1093/mnras/stac1438>
- 267 Lefèvre, M., Marcq, E., & Lefèvre, F. (2022). The impact of turbulent vertical mixing in the
268 Venus clouds on chemical tracers. *Icarus*, 386, 115148.
- 269 Mogul, R., Limaye, S. S., Lee, Y. J., & Pasillas, M. (2021). Potential for Phototrophy in Venus'
270 Clouds. *Astrobiology*, 21(10), 1237–1249. <https://doi.org/10.1089/ast.2021.0032>
- 271 Mogul, R., Limaye, S. S., Way, M. J., & Cordova, J. A. (2021). Venus' Mass Spectra Show
272 Signs of Disequilibria in the Middle Clouds. *Geophysical Research Letters*,
273 e2020GL091327.
- 274 Sousa-Silva, C., Seager, S., Ranjan, S., Petkowski, J. J., Zhan, Z., Hu, R., & Bains, W. (2020).
275 Phosphine as a biosignature gas in exoplanet atmospheres. *Astrobiology*, 20(2), 235–268.
- 276 Trompet, L., Robert, S., Mahieux, A., Schmidt, F., Erwin, J., & Vandaele, A. C. (2020).
277 Phosphine in Venus' atmosphere: Detection attempts and upper limits above the cloud top
278 assessed from the SOIR/VEx spectra. *Astronomy & Astrophysics*, 645, L4.
279